LIDAR SENSING OF ATMOSPHERIC PRECIPITATION

A.I. Grishin, A.E. Zil'berman, and G.G. Matvienko

Institute of Atmospheric Optics,
Siberian Branch of the Russian Academy of Sciences, Tomsk
Received December 28, 1994

Results are presented of experimental investigation into the atmospheric precipitation characteristics by means of a correlation lidar. It has been found feasible to determine the complete set of characteristics of the zone of precipitation and to follow their spatiotemporal evolution from lidar returns. It is also shown that the light precipitation essentially increase the efficiency of lidar measurements of the wind velocity.

Weather and climate of different regions in many respects are determined by the characteristics of atmospheric precipitation, so its study is an urgent problem of atmospheric optics.

A lot of theoretical and experimental papers are devoted to the influence of precipitation on the optical characteristics of the atmosphere. The problems of interaction of electromagnetic radiation with spherical particles were considered in Refs. 1 and 2. The data on the coefficient of radiation extinction by rain droplets in visible and IR spectral ranges were presented in Ref. 3. Polyakova and Shifrin[4–6] carried out extensive cycle of experimental investigations of water–droplet precipitation and obtained empirical dependence relating the intensity of precipitation with the light scattering characteristics of the atmosphere.

Experimental investigations of precipitation with the use of lasers have been started relatively recently and are presented in Refs. 7 and 8. Rogachevskii[7] and Goryachev and Mogil'nitskii[8] investigated mainly the effects of laser radiation propagation under conditions of precipitation of various intensity and payed scarcely any attention to the study of the characteristics of precipitation. As for lidar measurements, precipitation is most often considered as a factor limiting the range and accuracy of measurements and sometimes making them impossible. Since the probability of precipitation is rather high in some regions, this fact imposes serious restrictions on possible practical application of lidars.

However, in processing of experimental data, it was found that under some conditions precipitation increases the efficiency of lidar sounding by increasing the range and accuracy of measurements. This is especially true for rain precipitation of drizzle and continual types whose intensity is no more than 1.5 mm/hour. Such precipitation is quite often encountered. In addition, lidar is capable of measuring the basic characteristics of rain precipitation, monitoring the dynamics of its development and evolution, and making supershort–term forecast of rainfall (for periods of 3–5 min).

The purpose of this paper is to investigate experimentally the basic characteristics of precipitation by means of a wind correlation lidar developed and operated at the Institute of Atmospheric Optics since 1990. The data presented here were obtained at the Institute of Atmospheric Optics during summer and fall of 1993 near Tomsk. As a rule, sounding was started under conditions of heavy cumulonimbus clouds when the probability of precipitation was quite high. Situations in which it did not rain during the experiment were excluded from data processing. The wind speed and direction in the layer from 100 m up to the lower boundary of a cloud layer were measured simultaneously with the rain parameters.

INSTRUMENTATION AND MEASUREMENT TECHNIQUE

The three–path lidar LISA–1 with vertical scheme of detection and ranging was used for measurements, so in this case the situations were analyzed in which precipitation was at the initial stage of its development and rain droplets did not reach the ground.

The lidar we used for field measurements carried out sounding of the atmosphere along a generatrix of a cone with vertical axis. A laser was switched on in three fixed positions during one scanning period, thus enabling us to obtain data from spatially separated volumes.

Lidar specifications:

Pulse energy, J	0.1
Wavelength, nm	532
Angular divergence, mrad	0.5
Receiving aperture, m	0.3
Number of sounded levels	128
Spatial resolution, m	10–20
Number of bits of analog–to–digital converter	8
Time of data collection, min	20–30

Processing of lidar signals was based on the spectral correlation technique.[9] High–frequency filtration and correction for trend were done in preliminary processing of time series of lidar signals. Then the cross–correlation and phase functions were calculated by the fast Fourier transform. The wind velocity was determined by two techniques, from the shift of maximums of cross–correlation functions and from the slope angle of the phase spectra.

Preliminary analysis of spatial and temporal series of lidar signals obtained in the rain showed the capability of measuring the precipitation parameters, i.e., the parameters in the atmospheric zone of precipitation. It is conventional in meteorology to characterize the precipitation zone by such parameters as shape, vertical and horizontal dimensions and boundaries, phase of development, velocity of motion, and structure. In experimental practice, the structure of the precipitation zone is described by the integral parameters: intensity, mm/h; water content, g/m^3; and, number density of precipitation particles, m^{-3}. The integral parameters were calculated from the measured precipitation microstructure, i.e., from the size distribution of precipitation particles and their velocity.

The rain microstructure parameters were estimated based on the fact that gravitational separation of rain droplets occurs during their sedimentation. Since the lidar was capable of obtaining cross–sections through precipitation zone, from spatial series of optical signals we

0235-6880/95/07 545-04 $02.00

can follow the movement of fore– and back fronts of the zone occupied by rain droplets. The rain droplets with maximum and minimum radii are concentrated at these fronts, respectively. The sedimentation velocity of different rain droplet fractions was estimated based on the comparison of the fore– and back front positions at different times, and then the maximum and minimum radii of the rain droplets in the zone were determined from the Hann–Kintzer curve.[10]

To describe the droplet size distribution, the fact was used that since the lidar scattering volume is small (several parts or units of cubic meters), comparatively small number of droplets (from several units to several hundreds, depending on droplet size) are localized within this volume at any time. Since the droplet size is approximately the same within the narrow (relatively to the whole rain zone) height range due to gravitational separation, the contribution of each droplet to lidar return signal is approximately the same within this height range. Therefore, the variance of lidar return signal from this layer is determined only by the number of droplets N and, hence, the variation coefficient W_H for the layer at the height H is determined as[9]

$$W_H = N_H^{-1/2} .$$

Thus, measuring the values of the variation coefficient for this layer, one can determine the number of droplets N_H in a unit volume. By finding the value N_H consequently for all rain layers, one can determine the droplet size distribution function $f(a)$. Knowing the microstructural parameters of the precipitation zone enables one to calculate its integral characteristics. The number density N, i.e., the number of particles in a unit volume, is calculated by the formula

$$N = \sum_{i=0}^{k} n_i(a_i) , \qquad (1)$$

where $n_i(a_i)$ is the number of particles of radius a_i in a unit volume.

The instantaneous rain intensity I, in mm/h, at the instant of sounding is determined by the expression:

$$I = 4/3\ \pi \sum_i a_i^3\, n_i\, V(a_i) , \qquad (2)$$

where $V(a_i)$ is the droplet velocity.

Analogously, one can calculate the water content of precipitation, i.e., the amount of water, in grams per cubic meter, in the rain

$$W = 4/3\ \pi \sum_i a_i^3\, n_i . \qquad (3)$$

The correlation between transparency and rain intensity was obtained in Ref. 5, with the correlation coefficient being equal to 0.95, and a conclusion was drawn that the precipitation intensity is the main factor contributing to the transparency in the rain zone. The correlation between the extinction coefficient of the optical radiation (α, km^{-1}) and the rain intensity (I, mm/h) is expressed by the empirical formula

$$\alpha = 0.21\ I^{\,0.74} . \qquad (4)$$

The relation between the rain intensity and the water content was also obtained in Ref. 5 in the form

$$W = 0.065\ I^{\,0.88} . \qquad (5)$$

Vertical extension and boundaries of the precipitation zone can be estimated by an analysis of spatial series of lidar signals; however, one can obtain these characteristics more accurately from the correlation matrix constructed for time series of lidar signals. The velocity of motion of the zone can be estimated from the measured wind velocity.

RESULTS AND ANALYSIS

Analysis of optical signals reflected by precipitation showed that the increase of the wind sounding efficiency is first of all due to the amplification of the fluctuation component of a signal. As shown in Ref. 11, the increase of the signal variation coefficient for systems, harnessing the correlation technique of data processing, leads to improvement of the signal–to–noise ratio and, hence, to longer sounding range. Thus, rain droplets are the natural tracers that indicate the direction and speed of motion of air mass in which they are localized. Limitations on the operating range of the precipitation intensity are caused by the fact that in the heavy rain the maximum of the size distribution function is shifted toward larger radii. Calculations show that for particles whose diameter is less than 0.25 mm the wind drift velocity is 7–10 times greater than the gravitation sedimentation velocity and, hence, rain droplets can be the tracers. In addition, as the precipitation intensity increases, the lower limiting height, from which one can measure the wind velocity, increases simultaneously. It is connected with the effects of horizontal and vertical separation of rain droplets.

The correlation and phase functions for 1.6 km sensing range are shown in Figs. 1 and 2. It is seen from Fig. 1 that the cross–correlation function is characterized by high correlation near the maximum (about 0.9) that ensures the high accuracy of measurements.

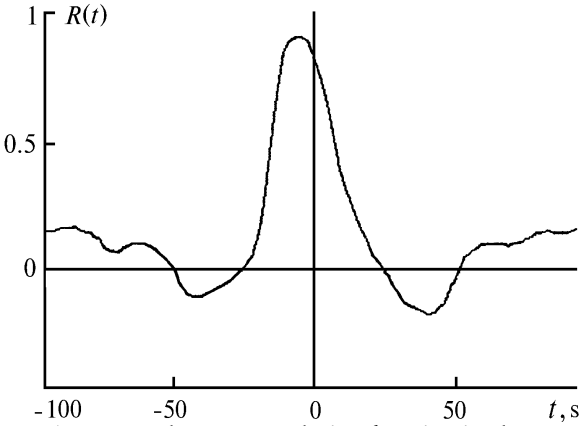

FIG. 1. Temporal cross–correlation function in the zone of precipitation on August 25, 1993.

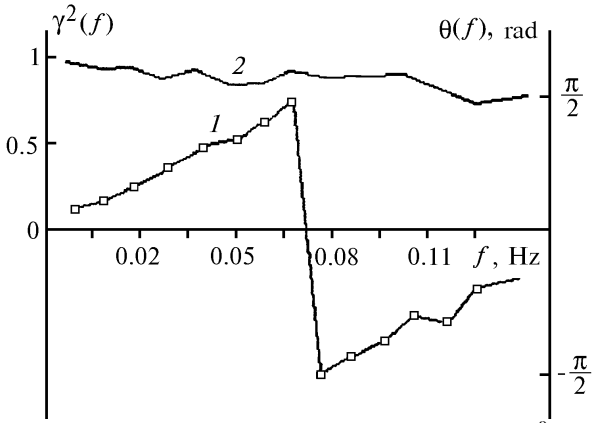

FIG. 2. Phase spectrum $\theta(f)$ and coherence spectrum $\gamma^2(f)$ in the precipitation zone. Measurement time is the same as in Fig. 1.

Analysis of the phase functions (curve *1*) and coherence functions (curve *2*) shows that the information–bearing frequency range essentially extends in the precipitation zone. As is seen from Fig. 2, the degree of coherence is at 0.8–0.95 level for the entire frequency range under investigation, and the phase function has the shape close to the classical one. This testifies high efficiency of measurements. At the same time, the fast decrease of the coherence level and, hence, narrower informative frequency range are observed out of the precipitation zone.

The vertical profiles of the wind velocity measured on August 25, 1993 are shown in Fig. 3. Horizontal bars indicate a confidence interval of 0.95. The data obtained were tested by means of a theodolite that measured the velocity of cloud motion (indicated by asterisks). In this case, the distance to clouds was determined from lidar return signals. As is seen from the figure, the data obtained at the lower boundary of clouds are in good agreement. As shown in Ref. 12, the wind shift in the precipitation zone, on the average, increases. This tendency can be followed in the figure.

The precipitation microstructure parameters were determined by the technique described above. The histogram constructed from the data averaged over 6 s intervals is shown in Fig. 4. It shows the number of particles n_i in each range of particle size a_i. The Khrgian–Mazin formula,[3] being the particular case of the gamma–distribution, was selected as an approximation for the precipitation particle size distribution function:

$$f(a) = A\, a^2\, e^{-\beta a}, \qquad (6)$$

where a is the droplet radius, A is the normalization factor, and β is the parameter.

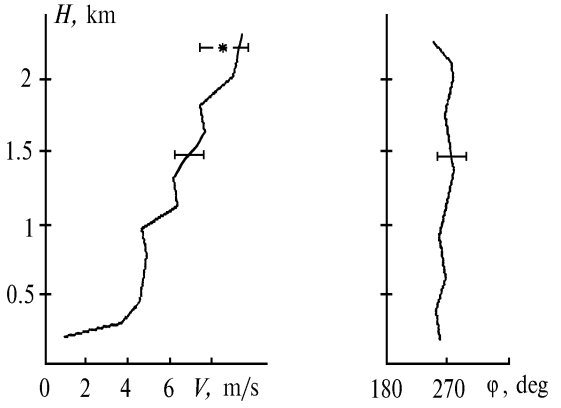

FIG. 3. Profiles of wind speed and direction in the rain.

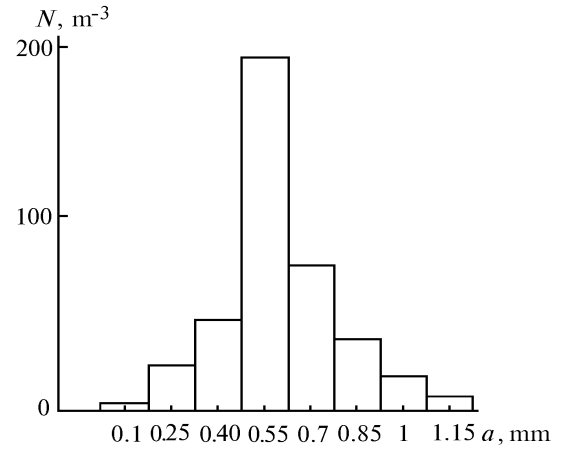

FIG. 4. Histogram of the rain droplet size distribution.

The parameters of distribution (6) were calculated by the technique proposed in Ref. 6. The comparison of the experimental distribution with the theoretical curve against the χ^2–criterion showed that the experimental distribution does not contradict the hypothesis that it is described by the curve calculated from Eq. (6) for a confidence probability of 0.95.

The number density of precipitation particles was calculated by Eq. (1) from the number of droplets in different size ranges. The other integral characteristics of the precipitation zone were calculated by Eqs. (2)–(5).

The measured microstructural data and the integral parameters determined from that data are presented in Table I.

TABLE I.

Date	Time	I, mm/h	W, g/m^3	α, km^{-1}	N, m^{-3}	r_{max}, mm	r_{min}, mm
25.08	18:25	7.7	0.39	0.9	388	1.3	0.1

Spatial boundaries of the precipitation zone were determined from the correlation matrices, as exemplified in Table II. Analyzing the matrix element values, we note that the correlation has a discontinuity at the levels corresponding to the fore– and back front positions that is explained by simple physical reasons. In addition, it is seen that the zone has a discontinuity in its vertical structure. This fact can be explained by the effect of separation of particles. The lower boundary of the zone is at a height of 1300 m, and the upper one – at 1700 m. Thus, the vertical extension of the zone during measurements was, on the average, 400 m. Since in meteorology the relative errors in determining the linear dimensions of the precipitation zone due to spreading of its transition zone are taken at a level of 30%, the result obtained may be considered as acceptable.

TABLE II.

H, m	1000	1100	1200	1300	1400	1500	1600	1700	1800	1900	2000	2100
1000	1.00	0.99	0.95	0.52	0.49	0.55	0.27	0.48	0.52	0.49	0.42	0.39
1100		1.00	0.97	0.52	0.53	0.59	0.28	0.54	0.57	0.54	0.47	0.44
1200			1.00	0.54	0.60	0.63	0.30	0.62	0.66	0.64	0.58	0.52
1300				1.00	0.24	0.29	0.42	0.21	0.28	0.26	0.21	0.15
1400					1.00	0.51	0.33	0.61	0.64	0.69	0.69	0.60
1500						1.00	0.66	0.59	0.61	0.57	0.50	0.43
1600							1.00	0.54	0.39	0.34	0.29	0.28
1700								1.00	0.93	0.85	0.78	0.74
1800									1.00	0.94	0.87	0.79
1900										1.00	0.97	0.88
2000											1.00	0.93

Based on the spatial series of lidar signals at different times, we may follow the spatiotemporal evolution of the precipitation zone from its origin (Fig. 5) and determine the time of the rain start that is usually estimated from falling of the first droplets on the ground. In addition, during measurements we have succeeded in predicting the rain 1.5–2 min before its start. Summing up, we note that precipitation considered as the natural tracer essentially enhances the efficiency of lidar measurements of the wind velocity. This is confirmed by the experimental results. However, the limitation is imposed on the precipitation intensity. At the same time, we may determine the complete set of characteristics of the precipitation zone and follow its spatiotemporal evolution from the spatial and temporal series of lidar

signals. In general, the technique for determining the precipitation parameters has not yet completely developed, and so further investigations in this field are necessary.

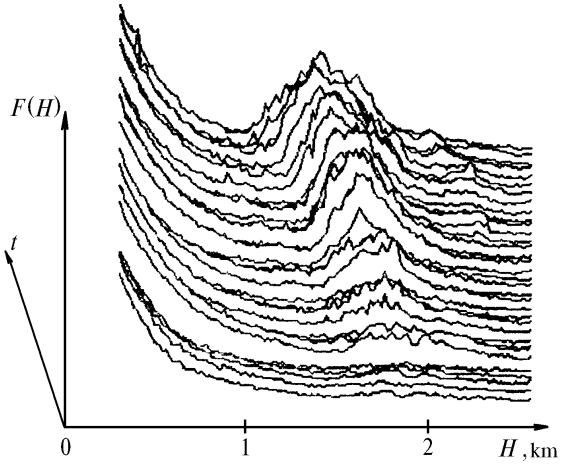

FIG. 5. Lidar signals recorded from the precipitation zone 2 s *apart.*

REFERENCES

1. D. Deirmendjian, *Electromagnetic Scattering on Spherical Polydispersions* (American Elsevier Publishing Company, Inc. New York, 1969).
2. H.C. van de Hulst, *Light Scattering by Small Particles* (J.Willey, New York – London, 1956).
3. V.E. Zuev, *Atmospheric Transparency for Visible and IR Radiation* (Sov. Radio, Moscow, 1966), 318 pp.
4. E.A. Polyakova, Tr. Gl. Geofiz. Obs., No. 68, 92 (1957).
5. E.A. Polyakova, Tr. Gl. Geofiz. Obs., No. 100, 45 (1960).
6. E.A. Polyakova and K.S. Shifrin, Tr. Gl. Geofiz. Obs., No. 42, 84 (1953).
7. A.G. Rogachevskii, in: *Propagation of Optical Waves in Randomly Inhomogeneous Atmosphere* (Nauka, Novosibirsk, 1979), pp. 75–82.
8. B.V. Goryachev and S.B. Mogil'nitskii, *ibid*., pp. 83–89.
9. J.S. Bendat and A.G. Piersol, *Random Data: Analysis and Measurement Procedures* (Willey, New York, 1971).
10. A. Ishimaru, *Propagation and Scattering of Waves in Randomly Inhomogeneous Media* [Russian translation] (Mir, Moscow, 1981), Vol. 1, 280 pp.
11. A.I. Grishin and G.G. Matvienko, Izv. Akad. Nauk SSSR, Fiz. Atmos. Okeana **17**, No. 11, 1148–1154 (1981).
12. I.V. Litvinov, *Precipitation in the Atmosphere and on the Ground* (Gidrometeoizdat, Leningrad, 1980), 208 pp.